Supporting Information

Simultaneously Formed and Embedding-type Ternary $MoSe_2/MoO_2$/Nitrogen-doped Carbon for Fast and Stable Na-ion storage

Yuanxing Yun,[a] Jie Shao,*[a,c] Xuefang Shang,[b] Wei Wang,[a,d] Weibo Huang,[a] Qunting Qu*[a,d] and Honghe Zheng*[a,d]

Material Characterization. Scanning electron microscopy (SEM) images were obtained using Hitachi S-8010 equipment operated at 10 kV. TEM images were obtained using FEI Tecnai G-20 microscope. Energy dispersive X-ray spectroscopy (EDS) were conducted using JEM-2100F field emission electron microscope. X-ray diffraction (XRD) patterns were collected using PANalytical X'Pert PRO MRD diffractometer with Ni-filtered Cu *K*α radiation. Raman spectra were measured through JobinYvon LabRAM HR800 Raman spectrometer with an excitation wavelength of 514 nm. X-ray photoelectron spectroscopy (XPS) was performed using an ESCA Lab250 spectrometer with a twin-anode Al Ka (1486.6 eV) X-ray source. Elemental analysis (VARIO MICRO) and inductively coupled plasma optical emission spectroscopy (OPTIMA 8000, PerkinElmer) were used to analyze the exact chemical composition of the ternary phases.

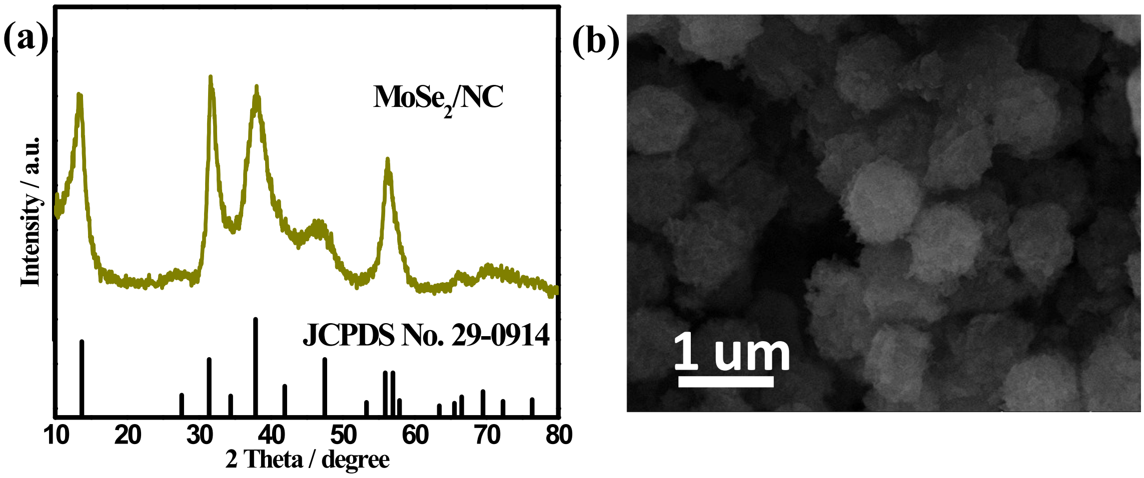

Figure S1 (a) XRD pattern and (b) SEM image of the as-prepared totally selenized binary phases $MoSe_2$/NC.

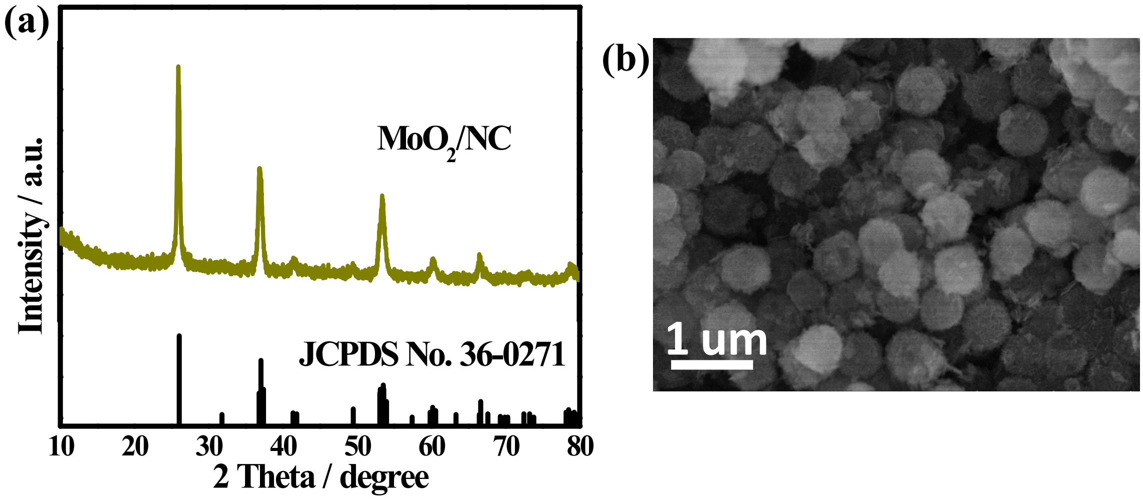

Figure S2 (a) XRD pattern and (b) SEM image of the as-prepared unselenized binary phases MoO_2/NC.

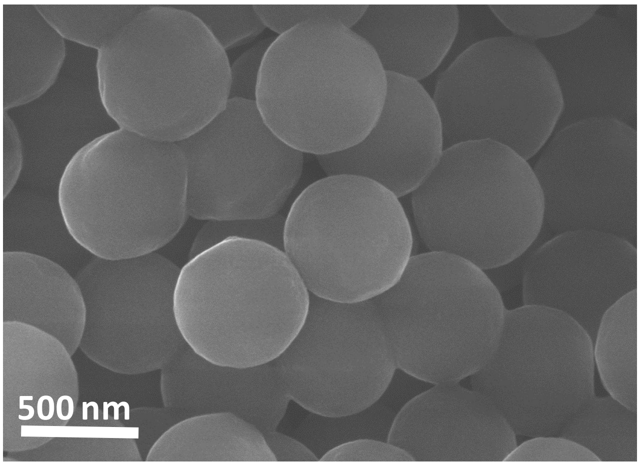

Figure S3 SEM image of pure SPS microspheres.

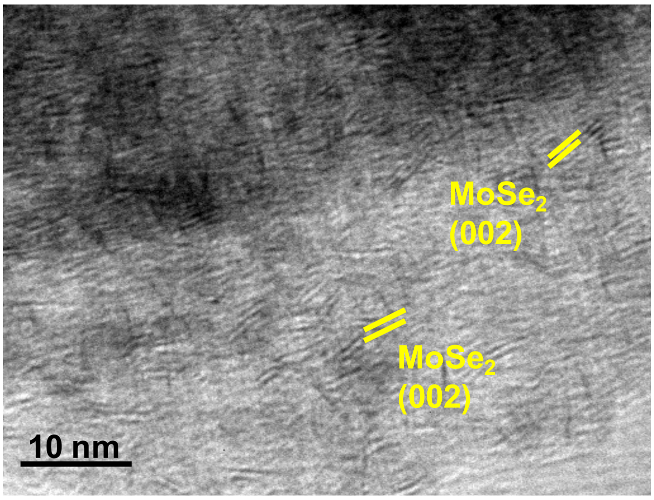

Figure S4 High-resolution TEM images of $MoSe_2/MoO_2$/NC.

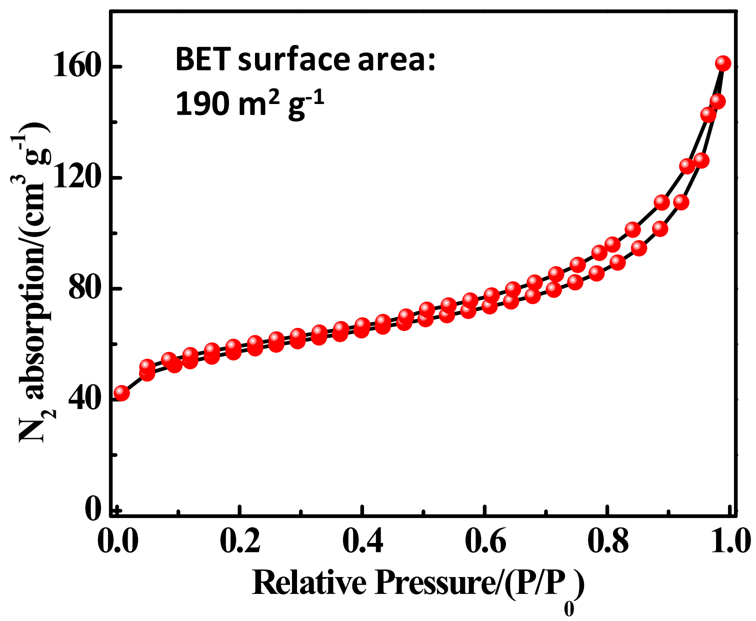

Figure S5 N_2 adsorption/desorption isotherms of $MoSe_2/MoO_2$/NC.

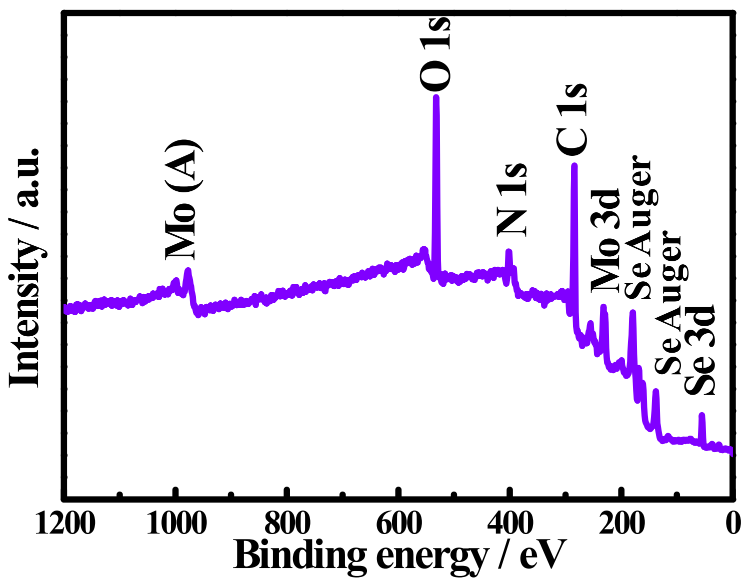

Figure S6 XPS survey spectrum of $MoSe_2/MoO_2$/carbon.

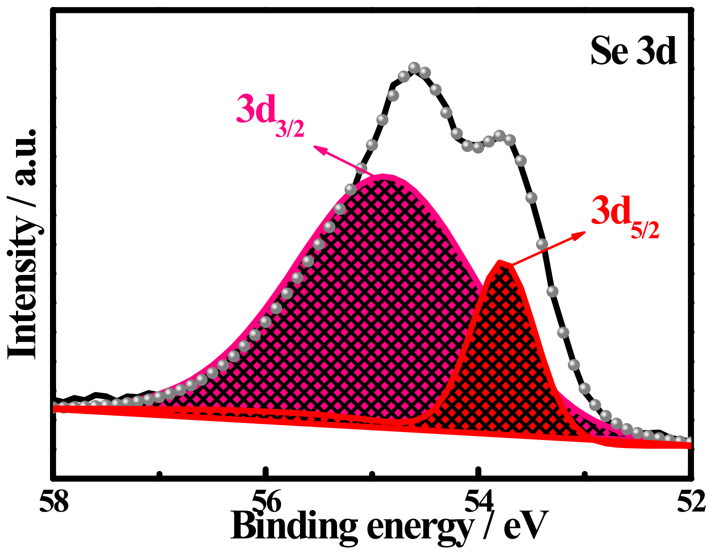

Figure S7 The deconvoluted XPS spectra of $MoSe_2/MoO_2$/carbon in the Se3d core level region.

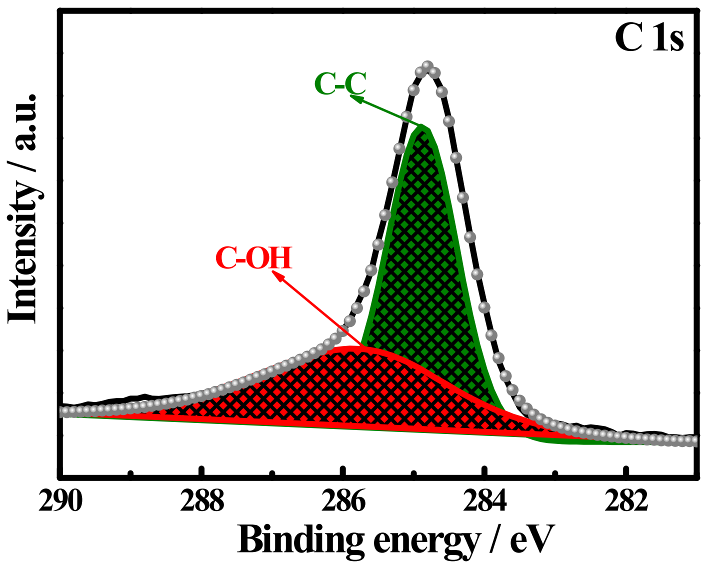

Figure S8 The deconvoluted XPS spectra of $MoSe_2/MoO_2$/carbon in the C1s core level region.

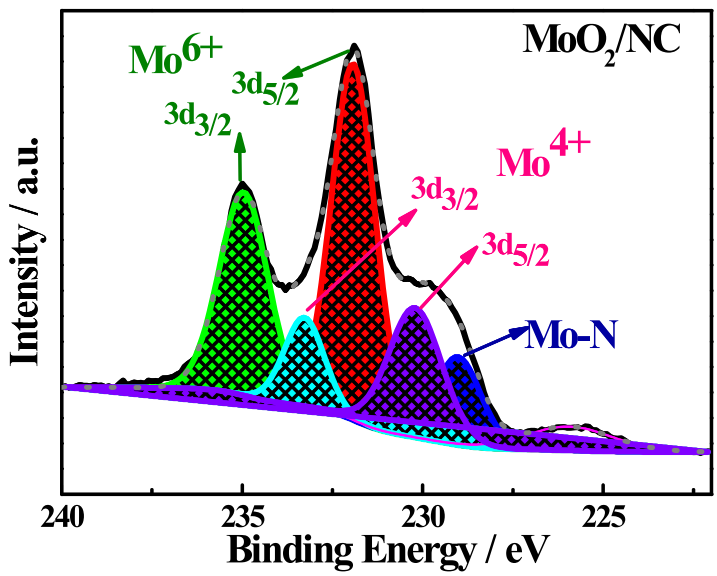

Figure S9 XPS spectra of binary MoO_2/NC in the core-level region of Mo3d.

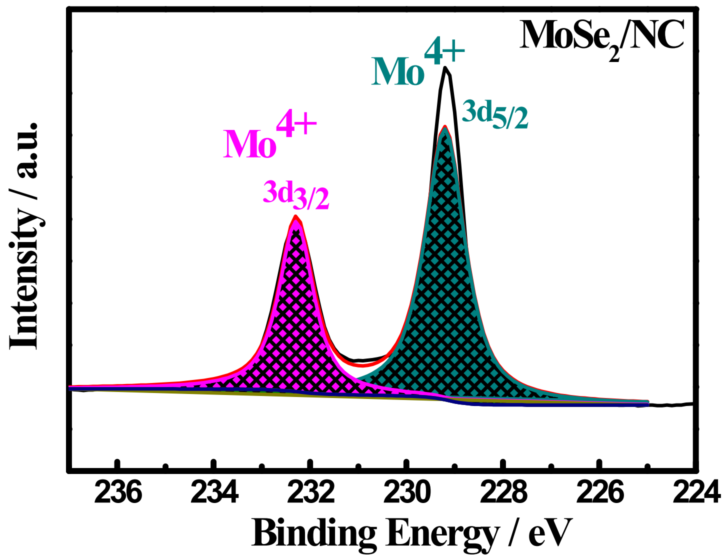

Figure S10 XPS spectra of binary $MoSe_2$/NC in the core-level region of Mo3d.

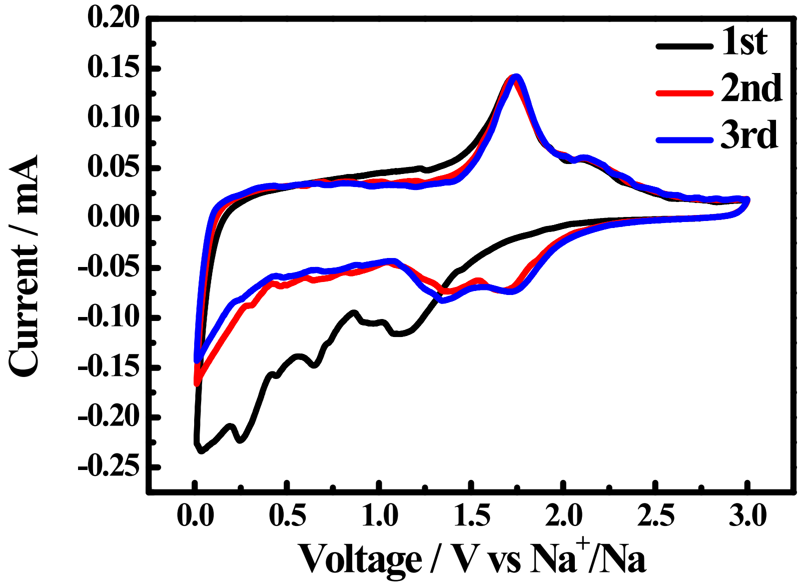

Figure S11 CV curves of the $MoSe_2$/NC electrode vs. Na^+/Na during the initial three scans.

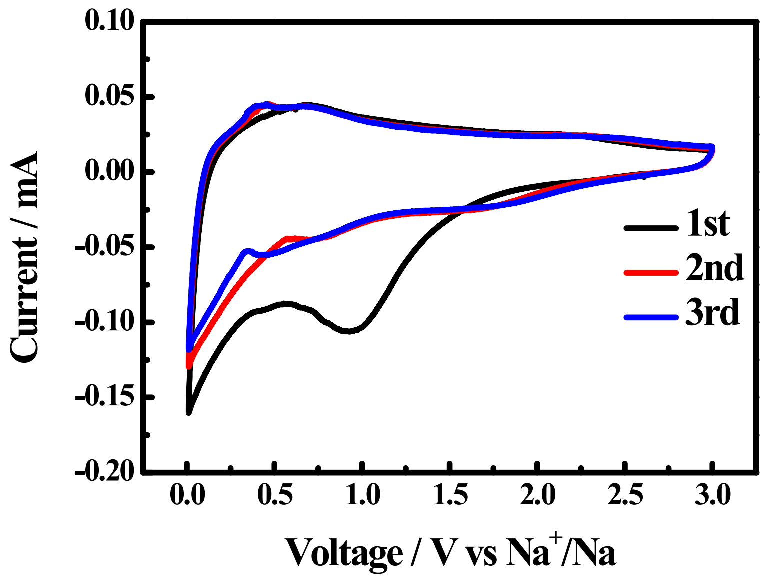

Figure S12 CV curves of the MoO_2/NC electrode vs. Na^+/Na during the initial three scans.

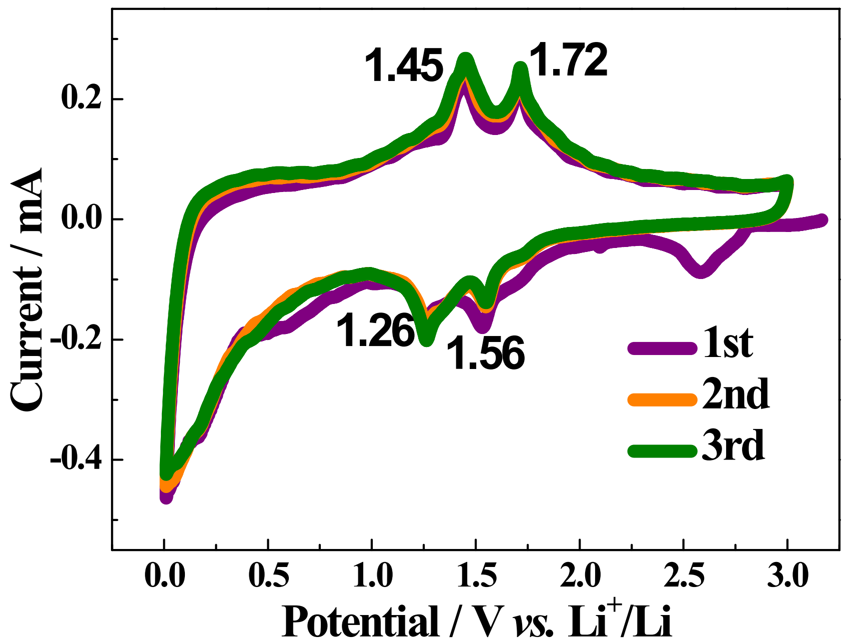

Figure S13 CV curves of the MoO_2/NC electrode vs. Li^+/Li during the initial three scans.

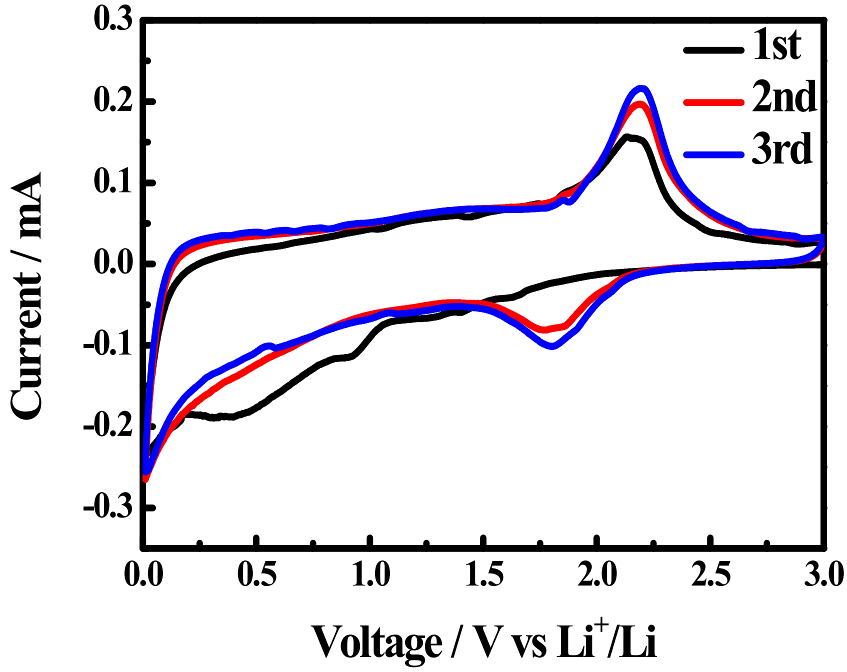

Figure S14 CV curves of the $MoSe_2$/NC electrode vs. Li^+/Li during the initial three scans.

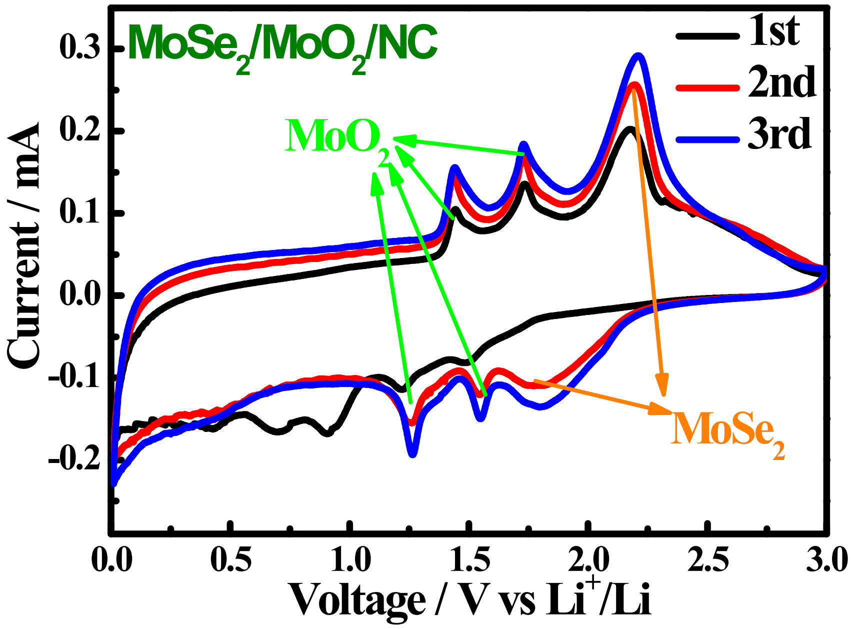

Figure S15 CV curves of the $MoSe_2/MoO_2$/NC electrode vs. Li^+/Li during the initial three scans.

Tab. S1 The mass percentages of all the elements in $MoSe_2/MoO_2$/NC.

Elements	C	N	Mo	O	Se
wt%	31.60%	1.80%	35.02%	6.72%	24.86%

Tab. S2 The electrochemical performance of some previously reported $MoSe_2$-based anodes for Na-ion batteries.

Materials	Initial capacity	Cycling performance	Rate behavior	Reference
N-doped carbon/scale-like $MoSe_2$	489.3 mAh g^{-1} at 0.5 A g^{-1}	378 mAh g^{-1} after 1000 cycles at 3 A g^{-1}	308 mAh g^{-1} at 10 A g^{-1}	1
$MoSe_2$/graphene	445 mAh g^{-1} at 0.1 A g^{-1}	358 mAh g^{-1} after 50 cycles at 0.4 A g^{-1}	324 mAh g^{-1} at 3.2 A g^{-1}	2
$MoSe_2$ nanotubes	304 mAh g^{-1} at 0.05 mA g^{-1}	228 mAh g^{-1} after 1500 cycles at 1 A g^{-1}	200 mAh g^{-1} at 2 A g^{-1}	3
$MoSe_2$/N-doped carbon microsphere	400 mAh g^{-1} at 0.1 A g^{-1}	138.6 mAh g^{-1} after 100 cycles at 1 A g^{-1}	61 mAh g^{-1} at 10 A g^{-1}	4
$MoSe_2$@CoSe/N-doped carbon	485 mAh g^{-1} at 0.1 A g^{-1}	347 mAh g^{-1} after 300 cycles at 2 A g^{-1}	392.8 mAh g^{-1} at 2 A g^{-1}	5
Carbon nanospheres encapsulated $MoSe_2$	498 mAh g^{-1} at 0.1 A g^{-1}	529 mAh g^{-1} after 120 cycles at 1 A g^{-1}	339 mAh g^{-1} at 5 A g^{-1}	6
$MoSe_2$@hollow carbon nanosphere	687 mAh g^{-1} at 1 A g^{-1}	471 mAh g^{-1} after 1000 cycles at 3 A g^{-1}	382 mAh g^{-1} at 10 A g^{-1}	7
$MoSe_2$/N,P-doped carbon nanosheets	454 mAh g^{-1} at 0.5 A g^{-1}	378 mAh g^{-1} after 1000 cycles at 0.5 A g^{-1}	216 mAh g^{-1} at 15 A g^{-1}	8
$MoSe_2$ nanosheets@ carbon	Around 600 mAh g^{-1} at 0.1 A g^{-1}	445 mAh g^{-1} after 100 cycles at 1 A g^{-1}	367 mAh g^{-1} at 5 A g^{-1}	9
$MoSe_2$/graphene/carbon nanotube	501.6 mAh g^{-1} at 1 A g^{-1}	335 mAh g^{-1} after 400 cycles at 1 A g^{-1}	173 mAh g^{-1} at 30 A g^{-1}	10
$MoSe_2$/MoO_2/N-doped carbon	634 mAh g^{-1} at 0.14 A g^{-1}	610 mAh g^{-1} after 1000 cycles at 2.1 A g^{-1}	461 mAh g^{-1} at 70 A g^{-1}	This work

References

1 H. Liu, B. Liu, H. Guo, M. Liang, Y. Zhang, T. Borjigin, X. Yang, L. Wang and X. Sun, *Nano Energy*, 2018, **51**, 639-648.

2 X. Zhao, W. Cai, Y. Yang, X. Song, Z. Neale, H.-E. Wang, J. Sui and G. Cao, *Nano Energy*, 2018, **47**, 224-234.

3 J. Zhang, M. Wu, T. Liu, W. Kang and J. Xu, *J. Mater. Chem. A*, 2017, **5**, 24859-24866.

4 C. Zhao, H. Song, Q. Zhuang, Q. Ma, J. Liang, H. Peng, C. Mao, Z. Zhang and G. Li, *Inorg. Chem. Front.*, 2018, **5**, 1026-1032.

5 J. Chen, A. Pan, Y. Wang, X. Cao, W. Zhang, X. Kong, Q. Su, J. Lin, G. Cao and S. Liang, *Energy Storage Materials*, 2019, **21**, 97-106.

6 P. Ge, H. Hou, C. E. Banks, C. W. Foster, S. Li, Y. Zhang, J. He, C. Zhang and X. Ji, *Energy Storage Materials*, 2018, **12**, 310-323.

7 H. Liu, H. Guo, B. Liu, M. Liang, Z. Lv, K. R. Adair and X. Sun, *Adv. Funct. Mater.*, 2018, **28**, 1707480.
8 F. Niu, J. Yang, N. Wang, D. Zhang, W. Fan, J. Yang and Y. Qian, *Adv. Funct. Mater.*, 2017, **27**, 1700522.
9 Y. C. Tang, Z. B. Zhao, Y. W. Wang, Y. F. Dong, Y. Liu, X. Z. Wang and J. S. Qiu, *ACS Appl. Mater. Interfaces*, 2016, **8**, 32324-32332.
10 G. D. Park, J. H. Kim, S.-K. Park and Y. C. Kang, *ACS Appl. Mater. Interfaces*, 2017, **9**, 10673-10683.